Self-Regulating Active Power Filter Compensation Scheme for Hybrid Photovoltaic-Fuel Cell Renewable Energy System for Smart Grid Applications

Adel A. A. Elgammal [1*], David Ali [2]

[1] SMIEEE, MIET, Department of Energy, the University of Trinidad and Tobago UTT, Point Lisas Campus, Trinidad and Tobago
[2] MPhil Graduated Student, the University of Trinidad and Tobago UTT

adel.elgammal@utt.edu.tt; davidali17@hotmail.com

[*] Corresponding author: adel.elgammal@utt.edu.tt

Received: 31.08.2016 Accepted:15.12.2016

Abstract: This paper presents a low cost DC and AC active power filters to enhance the power quality of hybrid hydrogen Fuel Cells (FC) and Photovoltaic arrays (PV) renewable energy system through reducing the complexity of design and control of active harmonic filters that effectively mitigate power system harmonics. Its main goal was therefore to design, model and test through computer simulation, active power filters that successfully interface FC and PV to form hybrid PV/FC renewable energy system that enhance the system output power quality through the stabilization of load bus voltage and reduction of harmonic currents. Two active power filters schemes were proposed in this paper. The first system consists of a unique two stage DC Power Filter (DCPF) to regulate the DC bus voltage to its set point. The second interface scheme is the active AC Power Filter (ACPF) which served to reduce harmonic three-phase currents on the AC bus. The AC filter used on the AC bus utilizes a hysteresis current controller to generate the switching. Computer models of these two interface schemes were built and simulation studies were carried out using the Matlab/Simulink. The simulation results demonstrate the success of both power filters at meeting their primary objectives through the increased voltage stability and reduction of the Total Harmonic Distortion (THD) of current that was observed as a result of their introduction into the power system.

Keywords: DC active power filter**,** Shunt Active Power Filter, Fuel Cell, Photo-Voltaic PV, Smart Grid Interface.

1. Introduction

Renewable energy is non-depletable, non-polluting and abundant in nature. In fact, renewable energy systems are gaining popularity for remote area power generation, especially in regions where grid extension is not feasible [1-2]. One downside of renewable energy sources is their low terminal voltage [3-4]. In general, renewable energy sources are unpredictable and inconstant nature and their variations do not match the time distribution of demand [5]. A hybrid energy system combines two or more renewable energy systems, an energy storage device, active power filter and a controller. Therefore The Hybrid Renewable Energy System (HES) benefit from their different energy sources, which allow a more constant power output when compared to systems employing each of the individual sources [6]. Despite the improvements in constancy of supply with HRES, the continual variability of renewable energy sources, coupled with the use of interfacing power converters that are necessary to meet the specific requirements of the power system's load, introduce unwanted power system harmonics. These harmonics pollute the power supply causing distortions in the voltage and current waveforms resulting in negative effects for all loads that are connected to the system [7]. For these reasons, power conditioning units (PCUs) comprising of passive and active filters and harmonic current compensators, form an integral part of the power system. A well-designed PCU can effectively reduce harmonic distortions and voltage irregularities. Without doubt,

reduction of harmonics is essential to improving the efficiency of the power system. Thus, the problem of harmonic loss evaluation is of growing importance especially to the renewable power system industry due to its impact on operating costs and useful life of system components. The role of power filters, both passive and active; in mitigating system harmonics make them a necessary component of a renewable energy system [8-9]. Thus, further research on the presently complex design and control of power filters offers the potential to lower the cost of these components and by extension reduce already high overall renewable energy system costs. Several research papers have dealt with hybrid renewable energy systems involving fuel cells and solar power, as well as other renewable sources; the control of power flow in a hybrid fuel cell system using an intricate control system based on fuzzy logic to control two DC-DC converters and an inverter to achieve increased power system stability during voltage sags was studied in [10]. Although the research work in [11] was primarily focused on achieving a higher level of energy continuity through the use of different renewable energy sources and maximum power extraction, a proportional–integral controller was utilized to control a DC to AC inverter so as to minimize power system harmonics when feeding power to the grid. A system to provide power to the utility grid through the use of Artificial Neural Network control method that varied the duty cycle of 2 buck boost DC-DC converters was developed in [12], each connected to an energy source, with the goal of regulating the output DC bus voltage. A fuzzy logic control system was then used to control a DC-AC inverter that supplied power to the AC grid from the DC bus. *A* hybrid switched harmonic filter which utilized a proportional-integral tri-loop error driven controller was presented in [13], to stabilize the voltage output of a variable frequency and amplitude rectified voltage from a wave energy powered generator. Although this was shown to be effective, it was only tested with a very low power, low voltage system and no harmonic analyses were done on the results. It was noted that even though in the above papers considerable work was done on hybrid renewable energy systems including solar hydrogen fuel cell systems for different applications, none contained substantial work on the development of higher efficiency, lower-cost power conditioning units for these hybrid energy systems. For hybrid fuel cell energy systems, the power conditioning units commonly comprise DC/DC converters & DC/AC converters. In many systems, each power source is connected to a single DC/DC converter, with one converter responsible for DC bus voltage regulation and the other converters for power tracking and control. This allows the energy system to eliminate large deviations from the desired bus voltage level while delivering the required power to the load. This method has been applied to the transportation sector in various studies [14]-[17]. Additionally, this method has been applied to distributed generation systems in studies conducted by [18]-[19]. A smoothing capacitor was utilized in [20], together with an inductor connected through a single phase H-bridge topology to absorb the ripple current created by a three-phase inverter load in a DC traction drive system. A PI hysteresis controller connected to the filter controlled the injection of the inductor current into the DC bus which in turn, charges the smoothing capacitor. Through charging and discharging of the capacitor the system minimizes the ripple current. The authors concluded that even though the system was effective in simulations, it was impractical due to its size, weight, large inductor current and switching losses. A study on reducing harmonics in a rectified DC traction drive system load through the use of a shunt three-phase AC active power filter with a control system based on p-q theory was conducted in [21] which the authors reported to be successful in reducing the current distortion of the supply under such dynamic loading conditions. The p-q theory was used to determine the reference current. The authors explain that the filter functions by injecting negative harmonic currents. A hysteresis controlled DC active filter with a unique topology consisting of two legs with an inductor was presented in [22], a diode and a power switch connected in parallel to a DC capacitor. Unlike the above two papers, the controller in this study used a low pass filter to extract the DC component of the load current and obtains the compensation current reference through calculation of the error between this current and the measured load current. According to the author, through simulation and experimental results, the system provides good compensation for the low-frequency ripple current that is produced by its aircraft inverter load application. Comparison of several DC-link active power schemes before choosing an active filter with a simple half-bridge topology for a system with a single phase PWM rectifier load was introduced in [23]. The authors used a control strategy based on dual-loop deadbeat control and repetitive control to demonstrate through simulation, the effectiveness of this means of control in reducing second-order ripple voltage in the DC-link. A DC current controller using hybrid energy storage in the dc-link was presented in [24] for a 4-wire current source active power filter. The hybrid energy storage consisted of an inductor, a capacitor, two diodes and two controllable switching devices. The authors indicated that experimental results showed that their control strategy resulted in an increase in filter efficiency as well as a reduction in the required dc-link inductance. In summary, a review of the research conducted on renewable energy systems revealed several research papers that mostly dealt with issues surrounding voltage stability, power management, continuity of supply and maximum power extraction. Few papers dealt with harmonics in renewable energy systems, especially DC harmonics. Those that did dealt with mostly AC harmonics in conventional power

systems and not renewable energy systems. Research in renewable energy system harmonics studied relatively low voltage and low power systems. The solutions presented, though effective, were very complex and therefore their practical application could be costly. Although, the converters and power filters utilized as power conditioning units in the papers discussed/referenced above have several different designs and can perform well depending on their application, additional research is required to develop active filter/compensation schemes that utilize simple yet effective control methods and topologies with fewer components to be used with hybrid renewable energy systems to boost operational performance and reliability and reduce currently high system costs. They must be effective in reducing harmonics, for not just AC but DC systems as well and they must be able to regulate bus voltages for higher power higher voltage systems. The main objective of this paper is to design, model and test through simulation, active power filters (power conditioning unit) that successfully interface hydrogen fuel cells and photovoltaic arrays to form hybrid PV/Fuel Cell renewable energy systems that provide power of enhanced quality. The control mechanisms for the power conditioning units developed through this paper must be simple yet effective at minimizing load bus voltage fluctuations and harmonic currents. The hybrid renewable energy systems developed in this paper must be easily adaptable to different industries in Trinidad & Tobago. As such, load packages that are representative of industrial type electrical loads have been chosen for use in the system models. The paper is structured as follows; Section 2 introduced the standalone hybrid photovoltaic (PV) and fuel cell (FC) energy scheme feeding a simple network that represents a small industrial/village electrical load. Section 3 provides explanations of the proposed DC active filter and the AC active filter as well as an explanation of the proposed controllers. Section 4 presents the simulation results of a standalone hybrid photovoltaic (PV) and fuel cell (FC) energy scheme feeding a simple network that represents a small industrial/village electrical load. It includes two case simulations with and without the proposed control scheme for the DC active filter and AC active filter. Finally, the conclusions of this paper are presented in Section 5.

2. Hybrid Photovoltaic/Fuel Cell DC Power Scheme

Figure 1 shows the layout of the test network of the hybrid photovoltaic (PV) fuel cell (FC) energy scheme feeding a simple network representing a small industrial/village load comprising of the following:

- A 10kW linear resistive load simulating heating and lighting
- A 35kW non-linear DC load
- Three (3) 40kW DC motor drives (Dynamic non-linear loads)
- A non-linear DC to AC three-phase inverter that feeds a three-phase 150kVA AC load bus consisting of AC motor drive & a non-linear three-phase load.

Two interface schemes connected to different load packages have been developed and studied through computer simulation in the Matlab/Simulink environment. The first system consists of a single DC load bus connected to the PV and FC energy sources through a unique two stage DC Power Filter (DCPF). The first stage is a voltage boost circuit which utilizes an open loop control system with no feedback loop required. The second stage is a buck circuit which is controlled by a simple voltage error fed proportional integral controller that uses a pulse width modulator to generate the switching action for the buck circuit to regulate the DC bus voltage to its set point. The load bus voltage reference can be changed by the system operator if necessary. The second interface scheme is the same as the first, with an added DC to AC inverter that connects a three-phase AC load bus to the system. AC loads were connected to this bus through an active AC filter which served to reduce harmonic three-phase currents on the AC bus. The AC filter used on the AC bus utilizes a hysteresis current controller to generate the switching. The reference current for the controller was calculated by subtracting the fundamental load current from the measured load current. The input to the controller is therefore the harmonic content of the load current only. The controller outputs the switching signal for an IGBT inverter which is connected to two DC capacitors. The capacitors act as a voltage source and are used to inject the harmonic current required by the load into the system.

The DC power filter (DCPF) is connected in series between the DC sources but before the DC loads. the three-phase AC bus is powered by the hybrid photovoltaic fuel cell DC energy scheme through the DC-AC inverter. The following AC loads are connected to this bus:

- A three-phase 50kVA cyclic load
- A three-phase 100kVA AC Motor drive system

The total system load is therefore approximately 235kW. Six different electrical bus voltages are defined in this model:

- Fuel Cell Bus voltage, V_{FC}
- Photovoltaic Array voltage, V_{pv}
- Main DC Source Bus voltage, V_{d0}
- Main DC Load Bus voltage, V_{d1}
- Main AC Source Bus voltage, V_{sAC}
- Main AC Load Bus voltage, V_{loadAC}

The 150kW PV energy source is connected to the main DC source bus, Vd0, via a series connected diode to prevent reverse current flow. The 150kW FC energy source is connected to Vd0 but through a DC-DC converter which serves as a means of simple energy supply management. The

fuel cell's DC-DC converter reference signal depends on the output current of the PV array. Under normal PV operation, the fuel cell reference current reference signal is half the maximum load current. When the PV current drops to zero, the fuel cell reference current signal increases to the full value of the maximum load current so as to allow the fuel cell to power the full system load. It should be noted that the 150kW power rating of the FC refers to its nominal output power. The FC is however capable of supplying additional power up to its maximum operating point of 240kW. Each energy source can be easily connected or disconnected from the system via circuit breakers Sfc and Spv. Circuit breakers S1, S2, S3, S4 & S5 control the connection of the DC loads to the system. Circuit breaker, S6, controls the connection of the DC to AC inverter load to the network. The three-phase AC harmonic filter (ACPF) is introduced on the AC bus. The ACPF is connected in shunt just after the DC-AC inverter through a three-phase circuit breaker S7.

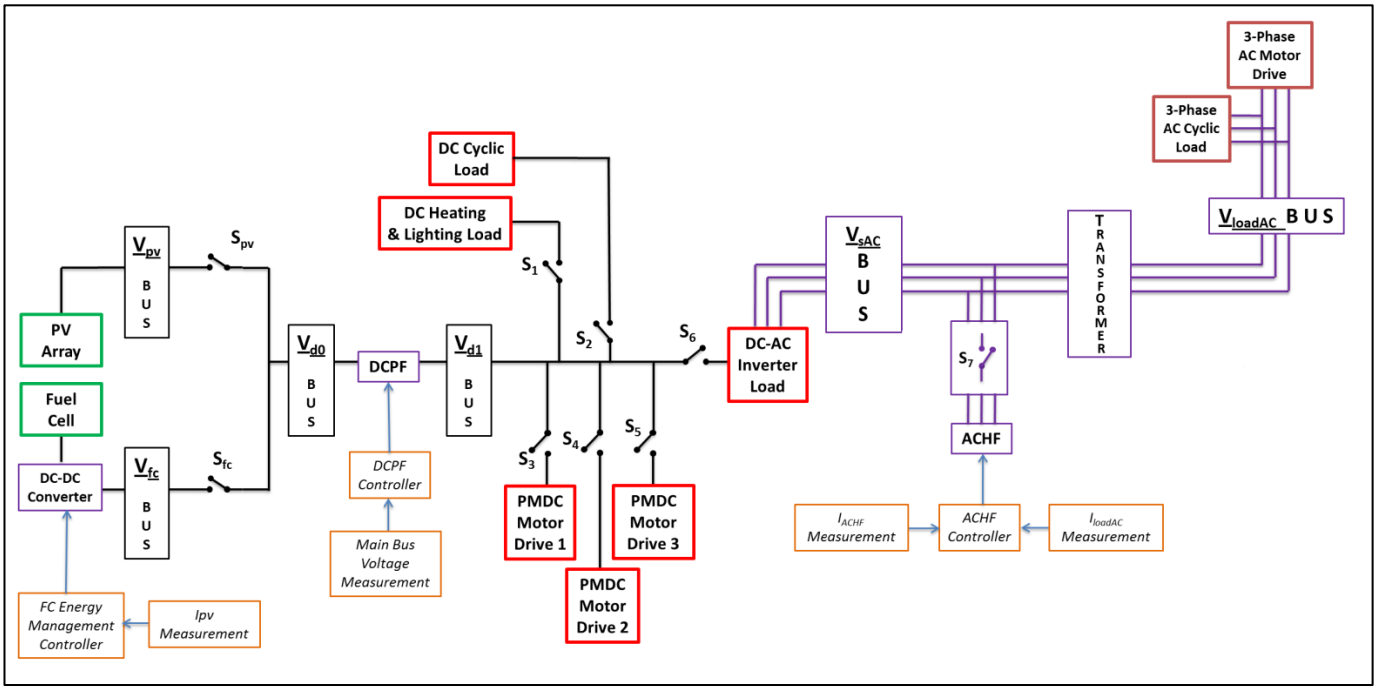

Fig. 1. Diagram of Hybrid PV-FC DC system with DCPF scheme & ACPF scheme

3. The Proposed Power Filters

Two schemes were used in this thesis, one designed for use with DC systems and the other for AC systems. The DCPF uses a unique approach to achieve its objectives which involves two stages, the first of which boosts the supply voltage to approximately three times the input and then the second stage which reduces the high voltage to the set point specified on the voltage controller. It is through this action that the filter is able to stabilize DC bus voltage and reduce harmonics. Each stage consists of a series of switches, resistors, capacitors & inductors arranged as shown in the figures (2) and (3). The DCPF main objectives are to regulate the DC load bus voltage and reduce the DC source current harmonics brought about by the connected loads. The DCPF device is connected as a DC–DC interface device between the dynamic DC load and the hybrid main PV and FC in order to achieve these objectives in the power system. The first stage comprises of an open loop controlled DC-DC boost circuit. The second stage of the DCPF reduces the boosted voltage to the required load bus value and maintains it at that value. This is achieved through the use of the error driven control system within the voltage controller block of the DCPF control system which comprises of a main voltage error loop. The error signal that is obtained by comparing the measured DC load bus voltage to the reference value of 500V is fed through a manually tuned proportional-integral (PI) controller. The output of the PI controller, which is also the output of the voltage controller is fed to a 50,000 Hz Pulse Width Modulator (PWM) which produces the signals, PWML & PWMH, that control the two switches of the second stage of the DCPF.

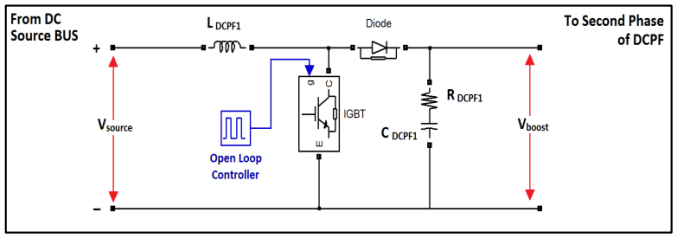

Fig. 2. Diagram of Stage 1 of DCPF

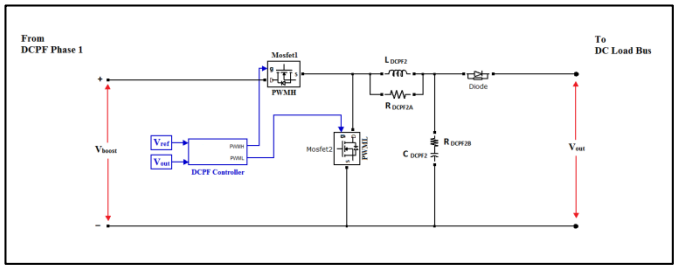

Fig. 3. Diagram of Phase 2 of DCPF

The ACPF is an active shunt filter that consists of two switched DC capacitors connected to a series inductor through a controlled IGBT three-phase inverter bridge. The ACPF controller is a simple yet robust current based controller that uses the AC load bus current measurement signal to generate a current waveform that matches the 60 Hz fundamental current required by the load. This generated current waveform is then subtracted from the measured load current to obtain the reference current which is equivalent to the harmonic current required by the load. The reference current is then fed to the hysteresis band controller which produces the switching signal that controls the connection of the filter elements to the system through the IGBT. The Simulink diagram in fig. 4 shows the layout of the ACPF .

The AC load bus current can be represented by the following equation:

$$I_{loadAC}(t) = I_{loadAC\_Fund}(t) + I_{loadAC\_Harm}(t) \quad (1)$$

Where I_{loadAC_Fund} represents the fundamental component of the load bus current and I_{loadAC_Harm} represents the undesired harmonic components of the load current that are required by the connected AC loads. Fourier analysis of an alternating current allows it to be broken down into several different sinusoidal waveforms each having a frequency which is a multiple of the fundamental frequency of 60Hz. This can therefore be applied to the AC load bus current resulting in the following equation:

$$I_{loadAC}(t) = \sum_{n=1}^{\infty} I_n \sin(n\omega t + \varphi_n) \quad (2)$$

In the above equation, n represents the harmonic order of the waveform which is a multiple of the fundamental frequency 60Hz. Therefore I_{loadAC} is a summation of all its harmonic components from the first to the infinite order, the first order being the fundamental component. Thus, I_{loadAC} can also be represented by the following equation:

$$I_{loadAC}(t) = I_1 \sin(\omega t + \varphi_1) + \sum_{n=2}^{\infty} I_n \sin(n\omega t + \varphi_n) \quad (3)$$

Where the fundamental component is

$$I_{loadAC\_Fund}(t) = I_1 \sin(\omega t + \varphi_1) \quad (4)$$

and the harmonic components are:

$$I_{loadAC\_Harm}(t) = \sum_{n=2}^{\infty} I_n \sin(n\omega t + \varphi_n) \quad (5)$$

The connected loads require both the fundamental component and the undesired harmonic components of the current. The AC source must provide all the current required by the connected. The main purpose of the ACPF is to reduce the harmonic content of the source current, leaving the fundamental component only. The ACPF accomplishes this by injecting a current equal to the harmonic current, into the system. The THD is utilized to compare and show the effectiveness of the proposed active filters. The THD is defined for voltages and currents, as:

$$THD_V = \frac{\sqrt{\sum_{n=2} V_n^2}}{V_1} \quad (6)$$

$$THD_I = \frac{\sqrt{\sum_{n=2} I_n^2}}{I_1} \quad (7)$$

Where

V_n = RMS voltage value of the harmonic n

V_1 = RMS voltage value of the fundamental current

I_n = RMS current value of the harmonic n

I_1 = RMS current value of the fundamental current

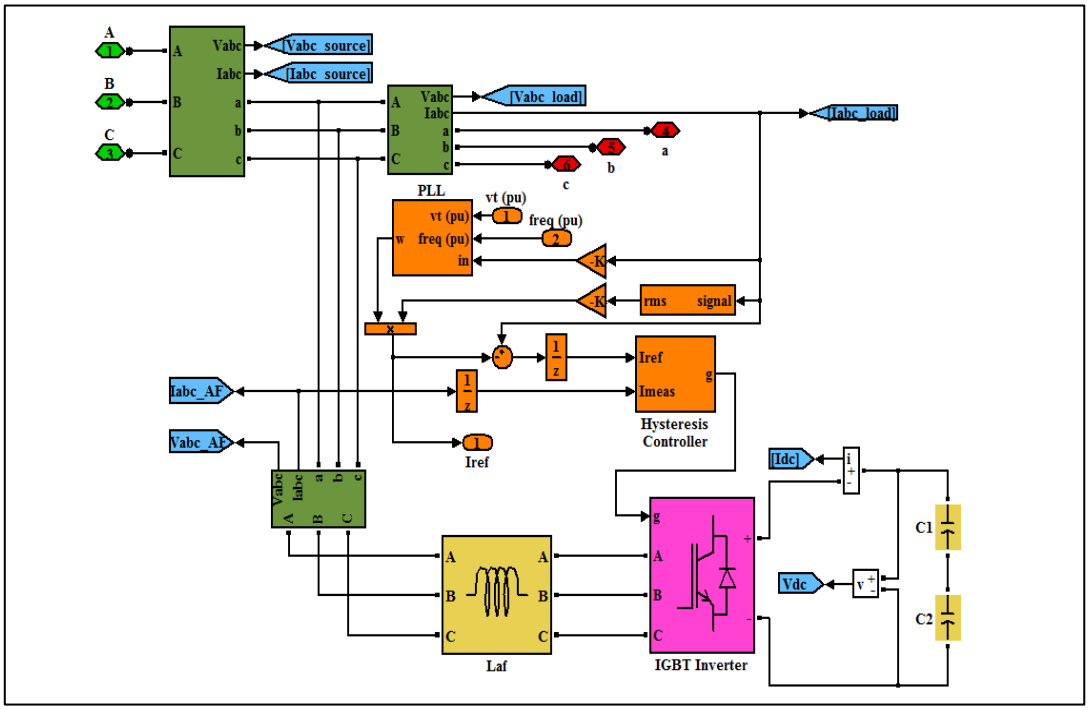

Fig. 4. AC Harmonic Filter (ACPF) Simulink model

4. Simulation Results

The simulation studies were carried out using the Simulink Version 7.7 which is part of the MathWorks Matlab Release 2011a software package. The effect of the ACPF primarily on the harmonic distortion of the AC source bus is analysed by closing S7 to connect the DC to AC inverter to the system. All other circuit breakers are closed except S4 & S5. In order to test the effectiveness of the ACPF scheme, the system performance is compared to an uncontrolled AC system, in which the ACPF is disconnected from the AC bus through the opening of circuit breaker S7. A system disturbance in the form of a two (2) second PV open circuit fault is introduced at simulation time t=2s. This is done by opening circuit breaker Spv at t=2s and then reclosing it at t=4s. The total simulation time for the model was 5 seconds. Through computer simulation it is observed that the AC power quality was significantly improved using the ACPF scheme. The effect of this scheme is compared to an uncontrolled case in which the ACPF is not connected to the system by opening circuit breaker S7. Through this comparison, the improvement in AC power quality is demonstrated using the simulation graphs and tables. The results show that utilization of the ACPF scheme results in significant improvements in power quality especially in terms of current harmonic distortion reduction. The effect of the ACPF is most evident through comparison of the THD of the AC source bus current (I_{sAC}) on simulations with and without the ACPF connected shown in Figure 5. In the uncontrolled case (represented by the red bars), the approximate steady state value of the THD of I_{sAC} is 27%, with an overall simulation average of 28.7%. Steady state is reached at approximately t=3s. The ACPF was able to significantly reduce the steady state THD to an average of just 5%, with an overall simulation average of 6.3%. This amounts to an 81% improvement in the steady state THD of the source bus current. The difference in current waveform shape can be seen through comparison of AC source bus current waveforms with and without the ACPF connected, as shown in Figure 6-a and Figure 6-b below. The current waveforms of the simulation with the ACPF shown in Figure 6-b are noticeably more sinusoidal in shape than the waveforms illustrated in Figure 6-a of the simulation without the ACPF, thus visually confirming the reduction in THD as a result of the ACPF. This improvement is possible through the ACPF controller's precise tracking of the filter reference current which enabled the ACPF to accurately inject the harmonic current required by the AC load bus. This is demonstrated in Figure 6-c below which shows the measured filter, depicted in black, current closely tracking the reference current, depicted in red. As table 1 clearly shows, a reduction in the steady state error of the AC load bus voltage (V_{loadAC}) and a substantial improvement of the THD of the AC source bus current (I_{sAC}) were attained through use of the ACPF . The ACPF, as well, have a significant effect on the THD of the source (V_{sAC}) and load bus (V_{loadAC}) voltages.

In order to test the effectiveness of the DCPF scheme, the system performance is compared to the uncontrolled system in which the DCPF and controller are absent. A system disturbance in the form of a two (2) second PV open circuit fault is introduced at simulation time t=2s. This is done by opening circuit breaker Spv at t=2s and then reclosing it at

t=4s. The total simulation time for the model was 5 seconds. Figures 7 and 8 show the increased voltage stability in both the load (V_{d1}) and source (V_{d0}) buses as a result of the installation of the DCPF. As with the previous case, this is most evident during the simulated PV open circuit fault between t=2s and t=4s. At the start of the fault an initial voltage drop of approximately 50V to a voltage of 450V was observed in the uncontrolled case (no DCPF connected). This voltage drop was completely eliminated through the introduction of the DCPF. It was also observed that in the uncontrolled case, the load bus voltage fluctuated between approximately 410 & 494V during this period. This is equivalent to a – 1% to -18% error from the 500V load bus rating. The addition of the DCPF significantly reduced the voltage fluctuation to a mere +/- 2% of the 500V bus rating resulting in a minimal fluctuation with voltages ranging between approximately 490V to 510V. Approximately sixty (60) volt fluctuations occurred before the PV open circuit fault period in the uncontrolled case and gradually reduced to eighteen (18) volt fluctuations at t=1.5s, with a maximum voltage value of 562V, thus yielding a maximum voltage error of approximately 12%. The DCPF was able reduce these fluctuations to +/-10V thereby achieving a steady state error of only +/-2%. Twenty (20) volt variations were observed after the PV fault in the uncontrolled case with fluctuations between 516V and 496V. The DCPF was also able reduce these fluctuations to +/-10V of the 500V bus rating. In fact, the load bus voltage graph shown in Figure 7-b shows no sign of the PV open circuit fault disturbance. Further comparison of the load bus voltage graphs of both cases at simulation start revealed similar settling times of approximately 1.5s to reach steady state, however, the voltage fluctuations in the uncontrolled case are remarkably larger than the case with the DCPF connected. Comparison of the source bus voltage graphs (Table 2) also revealed significant improvements in voltage stability. At the start of the PV fault, the DCPF reduced the initial voltage drop from a value of 450V in the uncontrolled case to a value of 466V, resulting in a 32% improvement. Throughout the fault period the DCPF reduced an 84V fluctuation with a maximum voltage of 494V and minimum of 410V in the uncontrolled case, to a 9V fluctuation with a maximum of 417V and a minimum of 408V, yielding an 89% reduction in fluctuation. Approximately sixty (60) volt fluctuations occurred before the PV open circuit fault period in the uncontrolled case and gradually reduced to eighteen (18) volt fluctuations at t=1.5s, with a maximum voltage value of 562V, thus yielding a maximum voltage error of approximately 12%. The DCPF was able reduce these 60V fluctuations to 9V fluctuations and was even able to eliminate the fluctuations by t=1.2s at which point the voltage was approximately 502V yielding a steady state error of 0.4%. The DCPF was also able to completely eliminate the twenty (20) volt fluctuations that were observed after the PV fault in the uncontrolled case, allowing the system to maintain a constant source bus voltage of 500V with no steady state error. Table 3 summarizes the reduction in the Total Harmonic Distortion (THD) of the load bus voltage that was brought about through the installation of the DCPF. Again, this improvement is most evident during the simulated PV open circuit fault between t=2s and t=4s. In the uncontrolled case, the THD of the DC load bus voltage during this period reaches an approximate average value of 14%. The table 3 illustrates the reduction of the THD of the load bus voltage to 4.3%, with the DCPF connected. The effect of the DCPF is also apparent in the first 0.6s of the simulation in which the THD is reduced from approximately 15% to 4.1%. The reduction in the Total Harmonic Distortion (THD) of the source bus voltage for the case with the DCPF scheme is illustrated as well in same table 3. In the uncontrolled case, the THD of the DC load bus voltage during the PV fault period reaches an approximate average value of 12% and reduced to 2.2 during this period. The effect of the DCPF is especially demonstrated through the comparison of total harmonic distortion of the source bus current graphs illustrated in table 3. It is clear that throughout the simulation, the THD of the source bus current was significantly reduced through the use of the DCPF. Before the PV fault, the total harmonic distortion exhibited a measureable improvement from a high of approximately 16% in the uncontrolled case to 2.6% with the DCPF until t=0.93s, after which it rose to only 2.8%. Another substantial improvement was noted during the PV fault period in which the THD dropped from a steady state value of approximately 17% in the uncontrolled case to 2.4% with the DCPF. After the fault period the system with the DCPF was able to reduce the steady state source bus current THD from 19% in the uncontrolled case to just 4.3%. **Error! Reference source not found.**9 and 10 show the increased voltage stability DC bus voltage as a result of the installation of the DCPF for sudden load between t=2s and t=4s. At the start of the sudden load change an initial load bus voltage drop of 490V to a voltage of 410V was observed in the uncontrolled case (no DCPF connected). This voltage drop was completely eliminated through the introduction of the DCPF. It was also observed that in the uncontrolled case, the load bus voltage fluctuated between 450 & 540V during this period. This is equivalent to a +/- 10% irregularity from the 500V load bus rating. The addition of the DCPF significantly reduced the voltage fluctuation to a mere +/- 2% of the 500V bus rating resulting in minimal fluctuation with voltages ranging between 490V to 510V. Twenty (20) volt voltage spikes were also observed before and after sudden load period in the uncontrolled case. The DCPF was able reduce these spikes by half to 10V. In fact, the load bus voltage graph shown in **Error! Reference source not found.** shows no sign of the sudden load disturbance. Further comparison of the load bus voltage graphs of both cases

(**Error! Reference source not found.** & **Error! Reference source not found.**) at simulation start revealed similar settling times of approximately 0.8s to reach steady state, however, the voltage fluctuations in the uncontrolled case are notably much larger than the case with the DCPF connected. **Error! Reference source not found.** & 12 show the difference in steady state voltage of the load (V_{loadAC}) bus that is brought about through the installation of the ACHF for a sudden load change. The voltage graph in **Error! Reference source not found.** for the uncontrolled case, shows that the AC load bus voltage reached a steady state value of approximately 425V at time t=2.8s, yielding a steady state error of 7.6% of the rated AC bus voltage of 460VRMS. The introduction of the ACHF resulted in a reduction of this error to 0.4% with an AC load bus steady state voltage of 462VRMS.

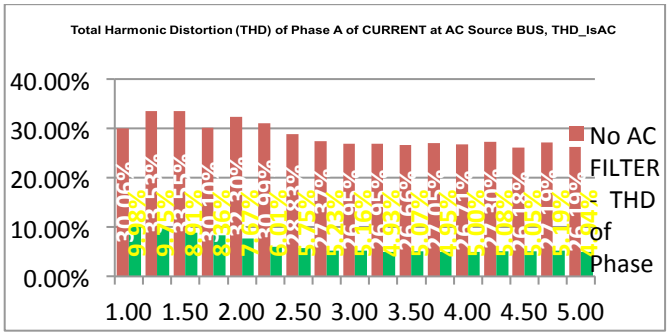

Fig. 5 Bar Graph comparing Total Harmonic Distortion of AC Source Bus Current, I_{sAC}, versus Time without & with ACPF scheme

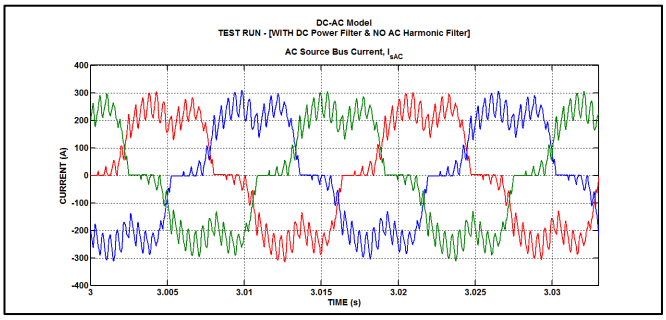

(a)

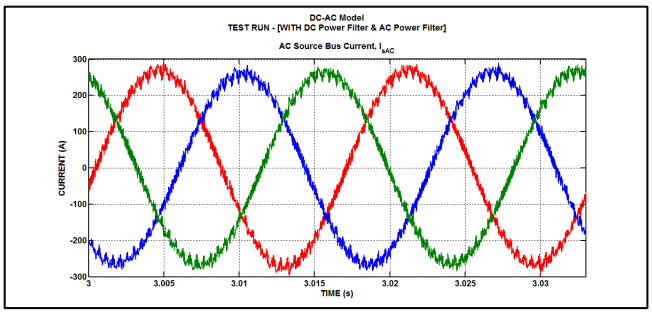

(b)

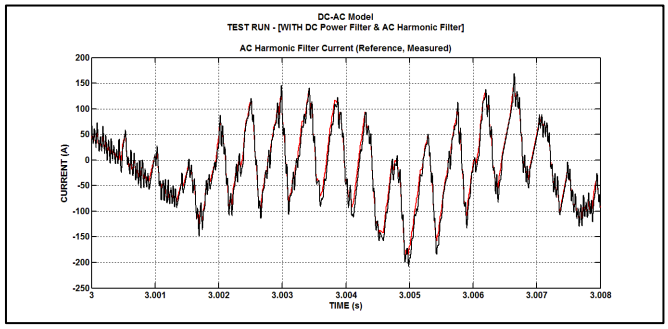

(c)

Fig. 6 Graph showing three-phase AC Source Bus Current, I_{sAC}, versus Time for simulation
(a) Without ACPF
(b) With ACPF
(c) Filter Current

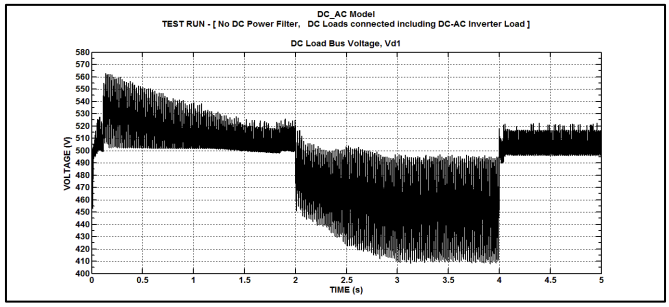

(a)

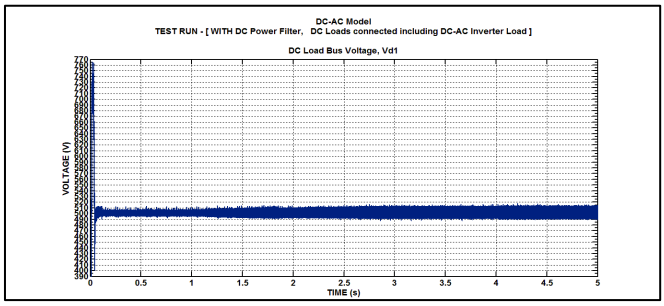

(b)

Fig. 7 Graph of DC Load Bus Voltage, V_{d1}, versus Time
(a) Without DCPF scheme
(b) With DCPF scheme

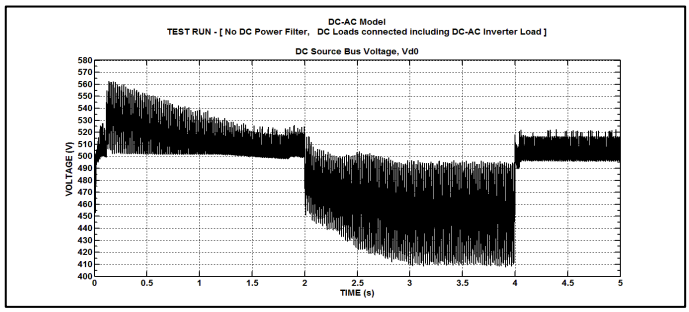

(a)

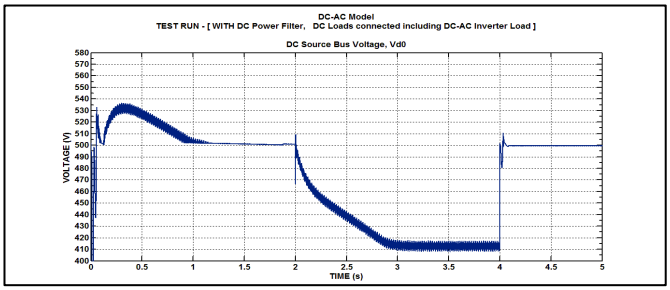

(b)

Fig. 8. Graph of DC Load Bus Voltage, V_{d0}, versus Time
(a) Without DCPF scheme
(b) With DCPF scheme

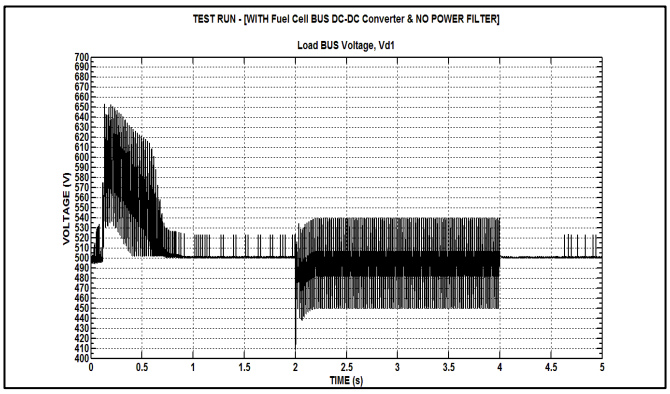

Fig. 9. Graph of DC Load Bus Voltage, V_{d1}, versus Time without DCPF scheme

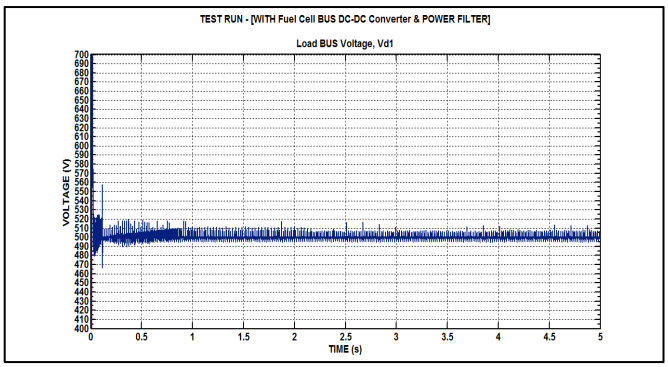

Fig. 10. Graph of DC Load Bus Voltage, V_{d1}, versus Time with DCPF scheme

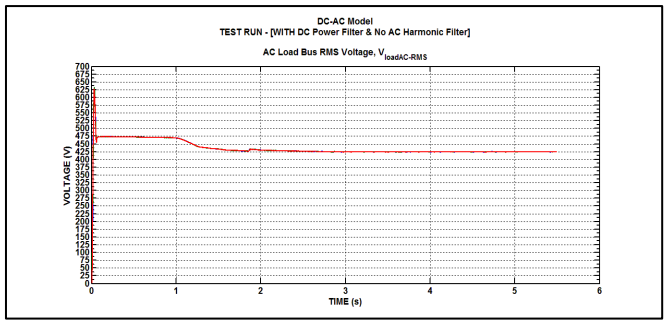

Fig. 11. Graph of AC Load Bus Voltage, V_{loadAC}, versus Time without ACPF scheme

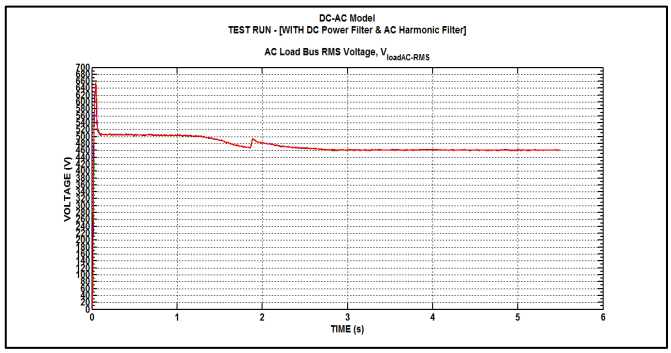

Fig.12. Graph of AC Load Bus Voltage, V_{loadAC}, versus Time with ACPF scheme

Table 1. Performance improvement summary with ACPF installation to AC Bus of Hybrid PV- FC system

	Steady State Error	THD			
	V_{loadAC} (RMS)	V_{loadAC}	I_{loadAC}	V_{sAC}	I_{sAC}
Without ACPF	7.6%	23%	29%	34%	29%
With ACPF	0.4%	4.9%	4.2%	4.5%	3.9%

Table 2. Performance improvement summary with DCPF installation of Hybrid PV-FC DC system with small industrial/village DC loads and DC-AC Inverter load

	Max. Fluctuation				Steady State Error			
	V_{d1}		V_{d0}		V_{d1}		V_{d0}	
Period	Normal Operation	During Disturbance	Normal Operation	During Disturbance	Normal Operation	During Disturbance	Normal Operation	During Disturbance

Without DCPF	20	84	20	84	+3% / -0.8%	-1% / -18%	+3% / -0.8%	-1% / -18%
With DCPF	10	20	0	9	+/- 2%	+/- 2%	0%	-1.7% / -1.8%

Table 3. THD improvement summary with DCPF installation of Hybrid PV-FC DC system with small industrial/village DC loads and DC-AC Inverter load

	THD							
	V_{d1}		V_{d0}		I_{d1}		I_{d0}	
Period	Normal Operation	During Disturbance	Normal Operation	During Disturbance	Normal Operation	During Disturbance	Normal Operation	During Disturbance
Without DCPF	14 %	15 %	12.3%	15 %	16.4 %	18.4 %	17.6 %	19.4 %
With DCPF	3.3 %	4.1 %	2.2 %	4.8 %	2.6 %	2.1 %	2.4 %	4.3 %

5. Conclusion

This paper has utilized two active power filters, the DCPF for DC power quality enhancement and the ACPF for AC power quality enhancement. Together with their accompanying controllers the DCPF and ACPF were able to improve the power quality of output of the hybrid PV-FC renewable energy system. The simulation results have demonstrated the effectiveness of the filters and their controllers. The size of the filter components along with the parameters of the controllers were optimized by trial-and-error through successive digital simulations. These simulations demonstrated the ability of both filters to significantly stabilize voltages and greatly reduce harmonic distortions. The success of both the PI controller for the DCPF and the hysteresis controller for the ACPF is unquestionable. In addition, through use of the Matlab/Simulink environment, a fully functional model of a hybrid PV-FC renewable energy system capable of powering a small industrial / village load has been developed. The power quality was significantly improved using the DCPF and ACPF schemes. The effect of these schemes is compared to an uncontrolled case in which the DCPF and ACPF are not connected to the system. Through these comparisons, the improvement in power quality is demonstrated using the simulation results. The results show that utilization of the DCPF and ACPF schemes results in significant improvements in power quality especially in terms of increased voltage stability and harmonic distortion reduction. This model can easily be implemented in several industries, including the manufacturing, telecommunications and transportation industries.

6. References

[1] Chih-Lung Shen; Po-Chieh Chiu"Buck-boost-flyback integrated converter with single switch to achieve high voltage gain for PV or fuel-cell applications" IET Power Electronics, 2016, Volume: 9, Issue: 6, Pages: 1228 - 1237,

[2] Sreeraj, E.S., Chatterjee, K., & Bandyopadhyay, S., (). "Design of isolated renewable hybrid power systems." Solar Energy, 2010, 84, 1124–1136.

[3] El-Sayed Ahmed, M., Orabi, M., AbdelRahim, O.M.: 'Two-stage micro-grid inverter with high-voltage gain for photovoltaic applications', IET Power Electron., 2013, 6, (9), pp. 1812–1821

[4] Krithiga, S., Gounder Ammasai Gounden, N: 'Power electronic configuration for the operation of PV system in combined grid-connected and stand-alone modes', IET Power Electron., 2014, 7, (3), pp. 640–647

[5] Deshmukh, M.K., & Deshmukh, S.S., (2008). Modeling of hybrid renewable energy systems. Renewable and Sustainable Energy Reviews, 12, 235–249.

[6] Gupta, A., Saini, R.P., & Sharma, M.P., (2006). Optimised application of hybrid renewable energy system in rural electrification. *Proceedings of India International Conference on Power Electronics, Chennai, India,* 337 - 340.

[7] Ramos, G., Cantor, E., Rios, M.A., & Roa, L.F., (2011). Instantaneous p-q Theory for Harmonic Compensation with Active Power Filter in DC Traction Systems. *International Conference on Power Engineering, Energy and Electrical Drives* (pp. 1-5),

[8] Yong Xu; Jingrong Yu; Yijia Cao; Xiaonan Lu; Jiaqi Yu "Double resonant output filter to eliminating the tradeoff between bandwidth and switching ripple in shunt active power filters" IET Power Electronics, 2016, Volume: 9, Issue: 4, pages: 846 - 854,

[9] Nguyen Duy Dinh; Nguyen Duc Tuyen; Goro Fujita; Toshihisa Funabashi "Adaptive notch filter solution under unbalanced and/or distorted point of common coupling voltage for three-phase four-wire shunt active powerfilter with sinusoidal utility current strategy" IET Generation, Transmission &

Distribution, 2015, Volume: 9, Issue: 13, pages: 1580 - 1596,

[10] Hajizadeh, A., & Golkar, M. A. (2010). Control of hybrid fuel cell/energy storage distributed generation system against voltage sag. Electrical Power and Energy Systems, 32, 488-497.

[11] Ahmed, N. A., Al-Othman, A. K., & Al-Rashidi, M. R. (2011). Development of an efficient utility interactive combined wind/photovoltaic/fuel cell power system with MPPT and DC bus voltage regulation. Electric Power Systems, 81, 1096-1106.

[12] Skretas, S. B., & Papadopoulos, D. P. (2009). Efficient design and simulation of an expandable hybrid (wind–photovoltaic) power system with MPPT and inverter input voltage regulation features in compliance with electric grid requirements. Electric Power System, 79, 1271-1285.

[13] Ozkop, E., Altlas, I. H., & Sharaf, A. M. (2012). A novel switched power filter-green plug (SPF-GP) scheme for wave energy systems. *Renewable Energy*, 44, 340-358.

[14] Zhang, X., Chunting Mi, C., Masrur, A., & Daniszewski, D., (2008).Wavelet-transform-based power management of hybrid vehicles with multiple on-board energy sources including fuel cell, battery and ultracapacitor. *Journal of Power Sources*, 185, 1533–1543.

[15] Thounthong, P., Chunkag, V., Sethakul, P., Davat, B., & Hinaje, M., (2009). Comparative Study of Fuel-Cell Vehicle Hybridization with Battery or Supercapacitor Storage Device. *IEEE Transactions on Vehicular Technology*, 58(8), 3892-3904.

[16] Thounthong, P., Raël, S., & Davat, B., (2009). Energy management of fuel cell/battery/supercapacitor hybrid power source for vehicle applications. *Journal of Power Sources*, 193, 376–385.

[17] Erdinc, O., Vural, B., Uzunoglu, M., & Ates, Y. (2009). Modeling and analysis of an FC/UC hybrid vehicular power system using a wavelet-fuzzy logic based load sharing and control algorithm. *International Journal of Hydrogen Energy*, 34, 5223–5233.

[18] Stewart, E.M., Lutz, A.E., Schoenung, S., Chiesa, M., Keller, J.O., Fletcher, J., Ault, G. McDonald, J. Cruden, A., (2009). Modeling, analysis and control system development for the Italian hydrogen house. *International Journal of Hydrogen Energy*, 34, 1638–1646.

[19] Thounthong, P., Raël , S., & Davat, B., (2008). Control Algorithm of Fuel Cell and Batteries for Distributed Generation System. *IEEE Transactions on Energy Conversion*, 23(1), 148-155.

[20] Shengnan Li, Ozpineci, B., & Tolbert, L.M., (2009). Evaluation of a Current Source Active Power Filter to Reduce the DC Bus Capacitor in a Hybrid Electric Vehicle Traction Drive *IEEE Energy Conversion Congress and Exposition* (pp. 1185-1190).

[21] Leonardo B. Garcia Campanhol; Sérgio A. Oliveira da Silva; Alessandro Goedtel "Application of shunt active power filter for harmonic reduction and reactive power compensation in three-phase four-wire systems" IET Power Electronics, 2014, Volume: 7, Issue: 11, 2825 - 2836,

[22] Zhong Chen, Miao Chen, Yingpeng Luo, & Changyou Wang, (2011). Low Frequency Ripple Current Compensation with DC Active Filter for the Single-Phase Aeronautic Static Inverter. *IEEE Energy Conversion Congress and Exposition* (pp. 1468-1475).

[23] Hongbo Li, Kai Zhang, & Hui Zhao, (2011). Active DC-Link Power Filter for Single Phase PWM Rectifiers. *IEEE 8th International Conference on Power Electronics and ECCE Asia* (pp. 2920-2926).

[24] Pettersson, S., Salo, M., & Tuusa, H., (2008). Optimal DC Current Control for Four-Wire Current Source Active Power Filter. *Twenty-Third annual IEEE Applied Power Electronics Conference and Exposition* (pp. 1163-1168).

7. Appendix: Model and Controller Parameters

Fuel Cell Parameters

Open Circuit Voltage (EOC) / V	Nominal Operating Current (Inom) / A	Nominal Operating Voltage (Vnom) / V	Maximum Operating Current (Iend) / V	Nominal Operating Voltage (Vend) / V
895	300	500	600	400

Photovoltaic Array Parameters

Number of Cells connected in Series, NS	Number of Parallel branches, NP	Cell Operating Temperature, TX / K	Solar Irradiation, SX / Watts/m2
655	800	293	100

DC Power Filter (DCPF) Parameters

DCPF Parameters – Phase 1

Filter series Inductance, LDCPF1 / H	Resistance, RDCPF1 / Ω	Capacitance, CDCPF1 / F	Pulse Generator Amplitude	Pulse Period / s	Pulse Width % of period
500e-6	0.05	15000e-6	1	50e-6	70

DCPF Parameters – Phase 2

Filter series Inductance, LDCPF2 / H	Resistance, RDCPF2B / Ω	Capacitance, CDCPF2 / F
500e-6	0.05	3000e-6

DCPF Parameters – Phase 2 Controller

PI Controller Proportional Gain, KP	PI Controller Proportional Gain, KI	PWM Generator Frequency / Hz	Pulse Width / % of period
0.5	200	50000	70

AC Harmonic Filter (ACHF) Parameters

Filter Inductance, LACHF / H	Capacitor 1, C1 / F	Capacitor 2, C2 / F	Switch Type	Hysteresis Band
0.1e-3	500e-6	500e-6	IGBT	0.01